Rabah ARARIA[1], Karim NEGADI[1], Mohamed BOUDIAF[2], Fabrizio MARIGNETTI[3]

Laboratory of L2GEGI, Department of Electrical Engineering, University of Tiaret (1)
Department of Electrical Engineering, University Ziane Achour of Djelfa (2)
Dipartimento di Automazione Università degli Studi di Cassino (3)

doi:10.15199/48.2020.03.20

Non-Linear Control of DC-DC Converters for Battery Power Management in Electric Vehicle Application

***Abstract**. In this paper, we use two DC/DC boost-buck converters powered a direct current motor. The boost converter ensures an energy flux for an ideal operation of the vehicle even in case of battery voltage drop. The buck converter his role is to controls and drives the electric motor at different operating conditions. To exploit the proposed approach in the automotive field, experimental tests were carried out. The performances obtained show the usefulness of this system for a better energy management of an electric vehicle and an ideal control under different operating conditions, mostly at nominal operation, in the presence of a load torque and even in case of battery chamber failure. The whole system has been tested experimentally using two microcontroller Arduino, We use Lyapunov nonlinear advanced control strategy and its performance has been analysed.*

Streszczenie.** W tym artykule wykorzystujemy dwa przekształtniki DC-DC typu boost-buck do zasilania silnika prądu stałego. Przekształtnik doładowania zapewnia strumień energii dla idealnej pracy pojazdu, nawet w przypadku spadku napięcia akumulatora. Jego rola polega na sterowaniu i zasilaniu silnika elektrycznego w różnych warunkach pracy. Aby wykorzystać proponowane podejście w branży motoryzacyjnej, przeprowadzono testy eksperymentalne. Uzyskane wyniki wskazują na przydatność tego systemu do lepszego zarządzania energią pojazdu elektrycznego i idealnego sterowania w różnych warunkach pracy, głównie przy pracy nominalnej, w obecności momentu obciążenia, a nawet w przypadku awarii celki akumulatora. Cały system został przetestowany eksperymentalnie przy użyciu dwóch mikrokontrolerów Arduino. Używamy nieliniowej zaawansowanej strategii sterowania bazującej na metodzie Lyapunova, a jego działanie zostało zilustrowano i przeanalizowane.* ***Nieliniowe sterowanie przekształtnika DC-DC w zarządzaniu napięciem baterii samochodu elektrycznego

Keywords: Electric vehicle (EV), DC-DC converters, Non linear controller, Lyaponov function, Permanent Magnet DC motor
Słowa kluczowe: Pojazd elektryczny (EV), przetworniki DC-DC, sterownik nieliniowy, funkcja Lyaponova, Silnik prądu stałego

Introduction

Electric Vehicles (EVs) are a solution for the environmental problems caused by vehicles with internal combustion engines. The advantages of EVs include energy efficiency, virtually lack of pollution, and the availability of electric energy through electric distribution systems. Among disadvantages, they have low energy density and long charging time for the present batteries. Hence, optimal energy management is very important in EVs [1]. The other major factors include optimum design of the motor, selection of a proper drive, and optimal control strategy [2, 3].

DC-DC converters are used to convert unregulated dc voltage to regulated or variable dc voltage at the output. They are widely used in switch-mode dc power supplies and in dc motor drive applications. In dc motor control applications, they are called chopper-controlled drives. The input voltage source is usually a battery or derived from an AC power supply using a diode bridge rectifier. These converters are generally either hard-switched PWM types or soft-switched resonant-link types [4, 5].

The dc/dc converter plays an important role in regulating the power flow in various system especially robots and electric vehicles. The battery bank voltage will vary with the operating conditions of the vehicle. Since the battery is directly connected to the main electrical node in the system it will make up the difference of current coming from the dc/dc converter and going into the motor drive [6, 7].

The structure of the presented work is organized as follow: the description of the proposed approach is set in section 2. The physical modelling and control of different part of our system with their equations model is set in section 3 and 4. The experimental results of the studied are presented in section 5. Section 6 summarizes the work done in the conclusion.

The proposed EV

The proposed schema is based on the electric traction system which contains a DC voltage source supplied by a battery, a DC-DC boost converter based MOSFET connected to a DC-DC buck converter controlled by the PWM technique and two electric permanent magnet MDC motor controlled by Lyapunov technique positioned behind the electric vehicle connected to the two wheels.

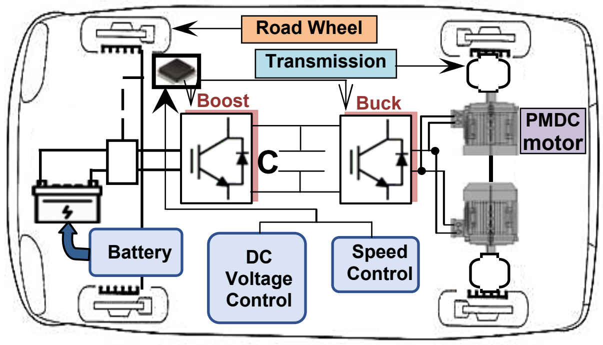

Fig. 1. Main components of the proposed EV

Firstly, the main objective is to control and regulate the speed and the DC voltage introducing the Lyapunov regulator and see the impact on the results obtained, and secondly the energetic aspect where the various curves at the exit of each element of the chain of traction were noted, notably the entry and the exit of the boost and the buck converter to confirm the feasibility and the high performances of the studied system. The schematic diagram above shows the components of the proposed system (Figure 1).

Mathematical Model of Permanent Magnet DC Motor

The DC motor has advantages over the AC motor. These advantages reside in the linearity of the mathematical model of the motor and the ease of setting up its control, the main interest of which is to eliminate the DC/AC conversion stage.

In addition, its model in the case of an experimental realization is supported by microcontrollers.

The system structure of a DC motor is depicted in Figure 2, according to the Kirchhoff's voltage law, the electrical equation of the DC motor is described as [8, 9]:

(1) $$V_c - R.i - L.\frac{di}{dt} - E = 0$$

(2) $$E = K_m.\Omega$$

where: R – the armature resistance, L – the winding leakage inductance, is the armature current, E – the buck electromotive force voltage, K_m [Wb.N.m.A^{-1}] is the velocity constant determined by the flux density of the permanent magnet, Ω [rpm] is the rotational velocity of the armature and U [V] is the voltage source .

Performing an energy balance on the system, the mechanical equation can be written as [8, 10]:

(3) $$T_e - J\frac{d\Omega}{dt} - F.\Omega - T_L = 0$$

Where, J – the inertia of the rotor and the equivalent mechanical load, F [N.m.rad/s] is the viscous friction coefficient, T_e [N.m] is the electromagnetic torque and T_L [N.m] is the load torque.

Putting the differential equations into state space form gives:

(4) $$\frac{d}{dt}\begin{bmatrix} i \\ \Omega \end{bmatrix} = \begin{bmatrix} -\frac{R}{L} & -\frac{K_m}{L} \\ \frac{K_m}{J} & -\frac{F}{J} \end{bmatrix}\begin{bmatrix} i \\ \Omega \end{bmatrix} + \begin{bmatrix} \frac{1}{L} & 0 \\ 0 & -\frac{1}{J} \end{bmatrix}\begin{bmatrix} U \\ T_L \end{bmatrix}$$

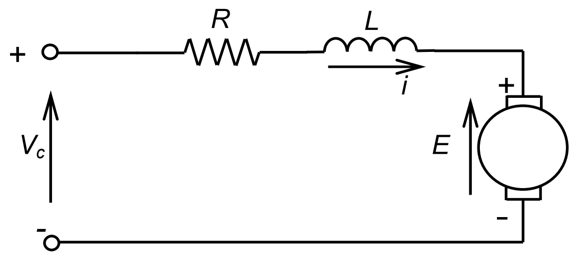

Fig. 2. Schematic of Permanent Magnet DC motor

DC/DC boost-buck Converters

The association of the two direct converters via a resonant stage will allow the correct operation of the battery (Charge / discharge). This association will also guarantee an adjustable tension and consequently ensure the variation of the speed.

The DC-DC converter acts as an interface between the system and the load. A boost buck converter is implemented here; it extracts the maximum power point regardless the state of charge of the battery and the constraints applied to the electric vehicle [11]. On changing the duty, cycle of the converter the source impedance can be matched with the load impedance to maximize the power efficiency. This converter either bucks or boosts the output voltage with respect to the input voltage. The boost buck converter is designed based on the following formulas: The output voltage of the converter [12, 13].

(5) $$V_c = V_{bat}\frac{D}{(1-D)}$$

For the design specification of the dc-dc boost buck converter parameters, the inductance L is given by:

(6) $$L_c = \frac{(1-D)^2 R}{2f}$$

Where: V_{bat} [V] is the input voltage battery, V_c [V] is the output voltage fed motor, D is the duty cycle of the converters, R [Ω] is the load resistance and f [kHz] is the switching frequency.

The voltage ripple of the boost buck converters is computed from [12, 14]:

(7) $$\frac{V_c}{V_{bat}} = \frac{D}{RCf}$$

The boost converter, which increases the battery voltage to desired output voltage as required by load. The configuration is shown in figure 3, which consists of a DC input voltage V_{bat} , inductor L , switch S, diode D, capacitor C for filter, and load resistance R .

When the switch S is ON the boost inductor stores the energy fed from the input voltage source and during this time the load current is maintain by the charged capacitor so that the load current should be continuous. When the switch S is OFF the input voltage and the stored inductor voltage will appear across the load hence the load voltage is increased. Hence, the load voltage is depends upon weather switch S in ON or OFF and this is depends upon the duty ratio D.

The power is connected to the DC voltage bus via the unidirectional boost-buck DC/DC converter, as shown in Figure 3.

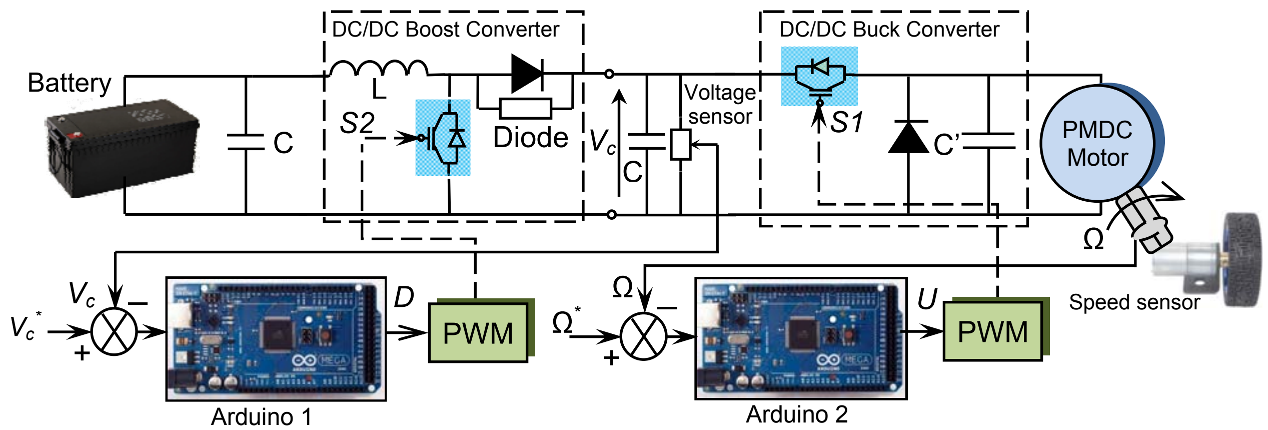

Fig. 3. Battery and DC/DC converters for electric vehicle control

The power system will operate in charging, modes depending on the energy requirements and this mode is managed according to the DC bus voltage at the point of coupling. Consequently, the power system is required to provide necessary DC voltage level under different operating modes of the vehicle.

During operation of the power electronics circuit, the switch S2 is activated and the converter operates as a boost circuit, and the switch S1 is activated and the converter operates as a buck circuit. When the voltage V_{dc} on the intermediate circuit is lower than the voltage reference, the Lyapunov regulator intervenes to increase it. The power budget of the intermediate circuit can be expressed by the following equation:

(8) $$P_{EV} = V_c i_c$$

where: P_{EV} : is the power of electric vehicle (W), i_c : is the current absorbed by the electric vehicle (A),

The objective of the boost converter is to maintain constant voltage at the DC link, so the ripple in the capacitor voltage is much lower than the steady-state voltage.

The Experimental System

The control strategy has been tested experimentally. A test bench has been set up for this purpose. The test bench shown in Figure 4 consists of:

- One Permanent Magnet DC motor with rated values shown in Table 1,
- Speed sensor for measure the speed of the motor,
- One DC-DC boost converter (based MOSFET),
- One DC-DC buck converter (based MOSFET),
- Two card Arduino Mega,
- DC power supply,
- Battery bank.

Fig. 4. Experimental setup

Parameters identification of DC motor and DC-DC boost

These parameters are determined experimentally from the figure 5 and 6.

DC motor

The gain :

$$k_m = \frac{\Omega_f(volts)}{u(volts)} = \frac{10}{12} = 0.83$$

Ω (Volts) : is the sensor output represents the image of the speed

τ_m : is the time constant, $\tau_m = 35$ ms

The transfer function of the motor can be written as:

(9) $$G(s) = \frac{k_m}{1+\tau_m s} = \frac{\Omega}{u}$$

(10) $$\Omega(1+\tau_m S) = k_m u$$

(11) $$\Omega + \tau_m \frac{\partial \Omega}{\partial t} = k_m u$$

The equation (11) represents differential equation of the system.

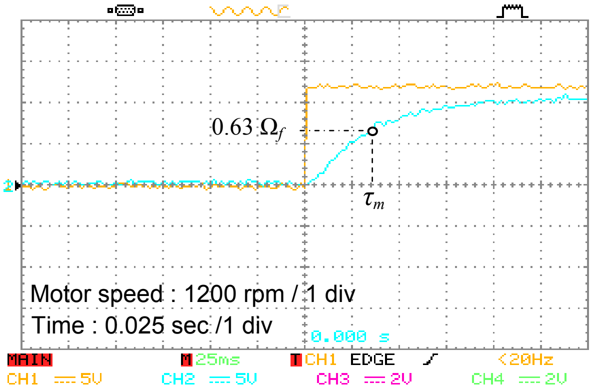

Fig. 5. The gain and the time constant of the DC motor.

Lyapunov Control DC motor

we put : $\Omega = x_1$

(12) $$\dot{x}_1 = -\frac{1}{\tau_m} x_1 + \frac{k_m}{\tau_m} u$$

(13) $$\dot{x}_1 = a.x_1 + b.u$$

along with : $a = -\frac{1}{\tau_m}$ and $b = \frac{k}{\tau_m}$

υ_m : the energy function of Lyapunov

We propose υ_m always positive and proportional with the norm.

so : $\upsilon_m(0) = 0$

Such as :

(14) $$\upsilon_m = \frac{1}{2} e^2$$

(15) $$\dot{\upsilon} = e\dot{e} < 0$$

To ensure the stability of the system, we put (16)

(16) $$\dot{e} = -\lambda_m e$$

with : $e = x_1^* - x_1$

(17) $$\dot{x}_1^* - \dot{x}_1 = -\lambda_m e$$

we replace equation (13) in (17); we obtain the following simplified equation:

(18) $$u = \frac{1}{b}\left[\dot{x}_1^* - \lambda_m \dot{x}_1 - (a+\lambda_m) x_1\right]$$

(19) $$u = k_0 u^*$$

where : k_0 : is the boost gain, λ_m : is the coefficient of adjustment of the boost.

(20) $$u^* = \frac{1}{bk_0}\left[\dot{x}_1^* - \lambda_m \dot{x}_1 - (a+\lambda_m) x_1\right]$$

$k_0 = \frac{12}{255} = 0.047$ and $\lambda_m = 100$

DC/DC Boost converter

The transfer function of the converter can be written as:

(21) $$F(s)=\frac{D}{1+\tau_c\cdot s}=V_c$$

(22) $$D=V_c(1+\tau_c\cdot s)$$

(23) $$D=V_c+\tau_c\cdot\frac{\partial V_c}{\partial t}$$

The equation (23) represents differential equation of the system

with: D : is the cyclical report, τ_c : is the time constant of the boost converter.

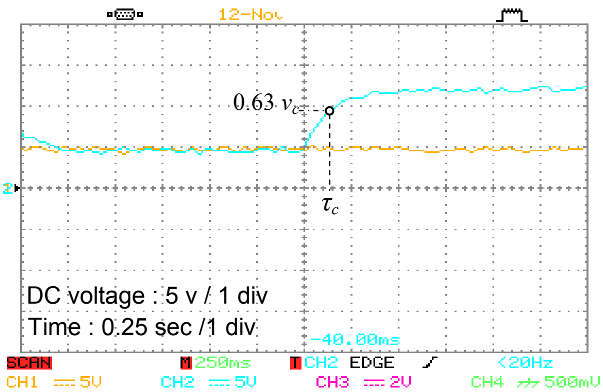

Fig. 6. The gain and the time constant of the boost.

Lyapunov Control of DC-DC Boost converter

we put : $V_c=x_2$

(24) $$\dot{x}_2=-\frac{1}{\tau_c}x_2+\frac{1}{\tau_c}D$$

(25) $$\dot{x}_2=-a_c x_2+a_c D$$

with : $a_c=-\frac{1}{\tau_c}$

υ_c : the energy function of Lyapunov

We propose υ_c always positive and proportional with the norm.

so : $\upsilon_c(0)=0$

Such as:

(26) $$\upsilon_c=\frac{1}{2}e_c^{\,2}$$

(27) $$\dot{\upsilon}_c=e_c\dot{e}_c<0$$

To ensure the stability of the system, we put:

(28) $$\dot{e}_c=-\lambda_c e_c$$

with : $e_c=x_2^*-x_2$

(29) $$\dot{x}_2^*-\dot{x}_2=-\lambda_c e_c$$

we replace the equation (25) in (29), we obtain the following simplified equation:

(30) $$D=\frac{1}{a_c}\left[\dot{x}_2^*+\lambda_c x_2^*+\left(a_c+\lambda_c\right)x_2\right]$$

where :

k_c : is the boost gain, λ_c : is the coefficient of adjustment of the boost.

$k_c=0.51$ and : $\lambda_c=200$.

The system control loop is shown in Figure 3.

Experimental Results and Discussions

The speed control has been verified experimentally to the test bench described in Experimental System. Practical tests were conducted on an electric vehicle equipped with a 60 W power Permanent Magnet DC motor. Numeric values of the motor and the DC-DC converter parameters are giving in the appendix. Experimental tests carried out are to assess the efficiency and dynamic performance of the proposed power management and control approach.

For the experimental results presented: 4 v / 1 div (DC voltage), 1200 rpm / 1 div (motor speed).

The performance of the proposed control is investigated by following tests on the Permanent Magnet DC motor drive.

Case study 1: Performance without boost converter

The battery voltage being at 12 V, in Figure 7 (a), the motor has been initially set to operate at 1490 rpm in steady state with no applied load. A sudden resistive load has been then applied at 0.3 s and removed at 0.7 s to the motor shaft (Figure 7 (b)).

According to these results, it should be noted that the measured speed follows its reference with a good response time and without exceeding

With a battery voltage of 9 V, the Figure 8 (a) show the waveform of the real speed and its reference, the measured speed does not follow its reference, neither the control system nor the buck converter manage to maintain the stable situation. Hence the need to insert a dc/dc boost converter.

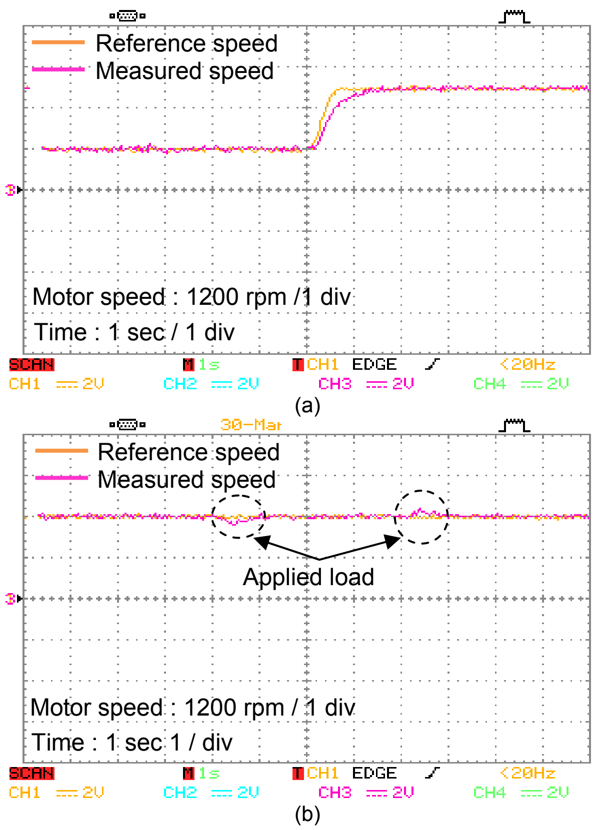

Fig. 7. Speed response, (a) without load, (b) with applied load. Vbat=12 V

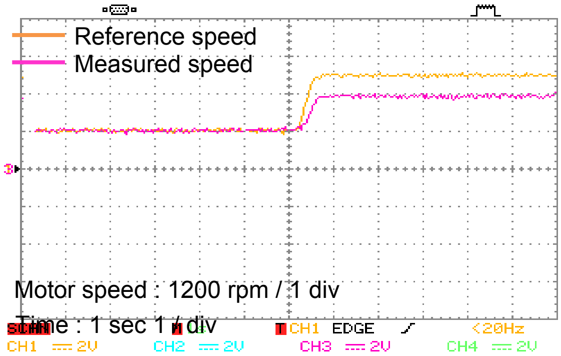

(a)

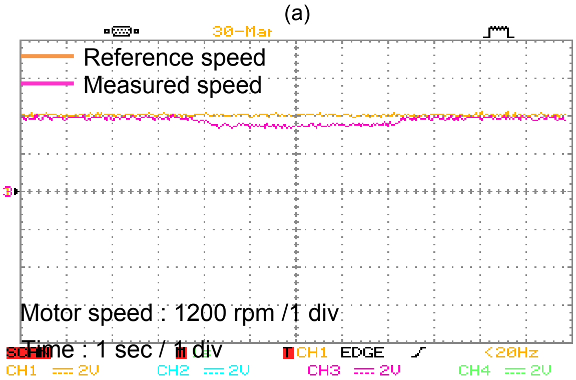

(b)

Fig. 8. Speed response when the voltage decreases, (a) without load, (b) with applied load. V_{bat}=9 V

Case study 2: Performance of the proposed system with boost-buck converters

No-load operation is presented in Figure 9; the system is powered with 12 V.

It is obvious that speed control can be performed even at start-up, which is considered a transient regime. The quality of speed control is shown in Figure 9 (a). Even good results have been obtained when applying a load torque (Figure 9 (b)).

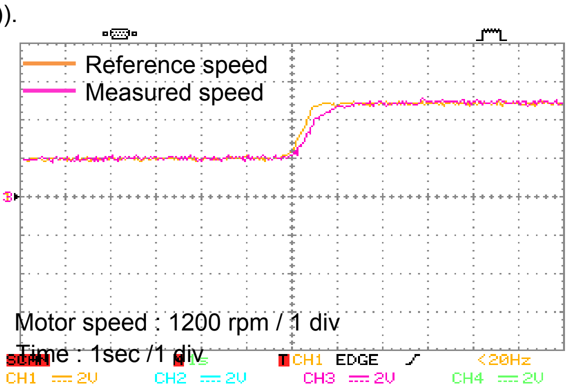

(a)

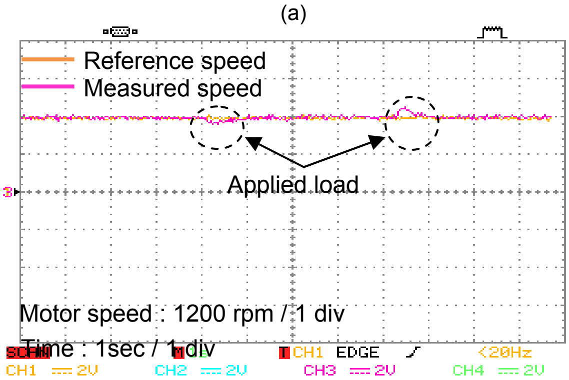

(b)

Fig. 9. Speed response, (a) without load, (b) with applied load. V_{bat}=12 V

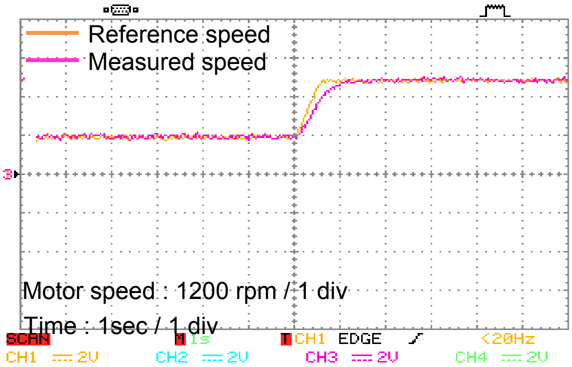

(a)

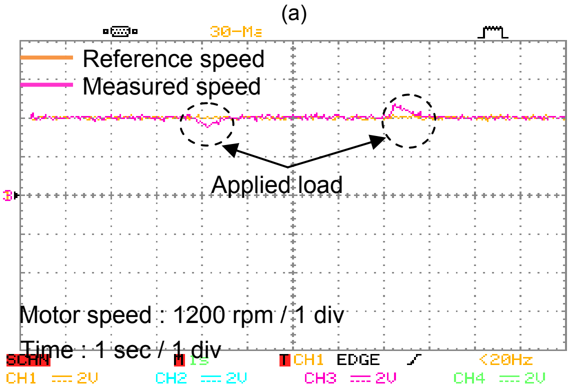

(b)

Fig. 10. Speed response, (a) without load, (b) with applied load. V_{bat}=9V

This test put the difference and shows the efficiency of the boost converter, the battery voltage is now at 9 V, the boost intervenes to put the buck converter a tension able to satisfy the speed control. The Figure 9 illustrated the speed response without applied load (a) and with applied load at 0.35 s and removed at 0.7 s, the reference speed and the measured one follow the target indicating the high performance of the proposed method.

With regard to the voltage regulation, it can be seen from figure 11 (a) and (b) that the measured voltage always follows the reference voltage even under steady state or transient conditions due to the variation of the load and this stability is ensured by the presence of the boost converter in the overall system.

No-load operation is presented in Fig. 10 - Fig. 11. The transient of speed in slow reversing is presented in Fig. 10. It is obvious, that the speed control can be performed even at very low frequencies. The quality of speed estimation is presented in Fig. 10. The estimation error is relatively low, having the peak at zero speed, as expected. Another important issue is the quality of torque tracking, presented in Fig. 10(b). The absence of torque sensor makes it impossible to measure the actual torque, thus only the desired and estimated values can be presented. It is obvious that regarding the high dynamics of the signal, the torque tracking is very good, as presented in Fig. 11. It has to be taken into account that every observer has the limited frequency range, which cannot he exceeded by the controller.

Figure 12 shows the experimental results of a battery failure scenario, it's meaning that the battery voltage will be degraded, according to this figure; the measured voltage dc always follows its reference with a slight disturbance of the fault. Therefore whatever the state of charge of the battery the boost converter keeps the voltage constant, it absorbs a current to make the compensation of the battery fault and that during a significant period seconds (figure 13 (a))

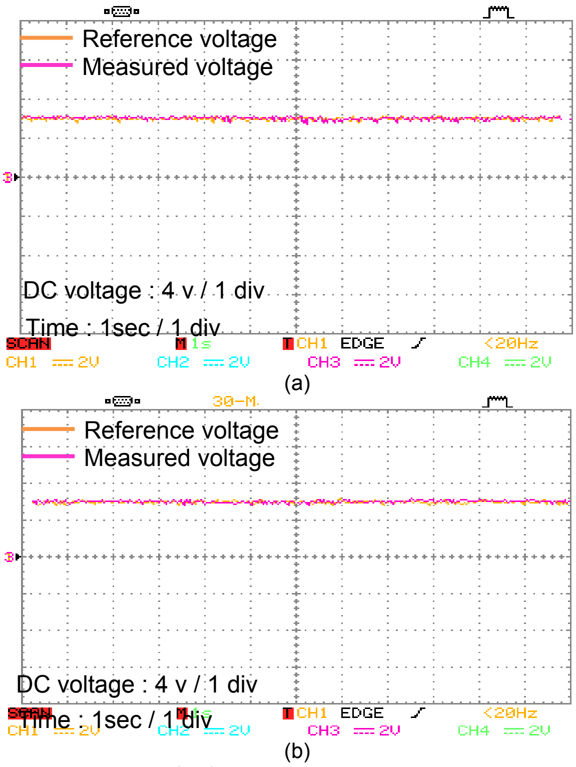

Fig. 11. Response of DC voltage control, (a) without load, (b) with applied load.

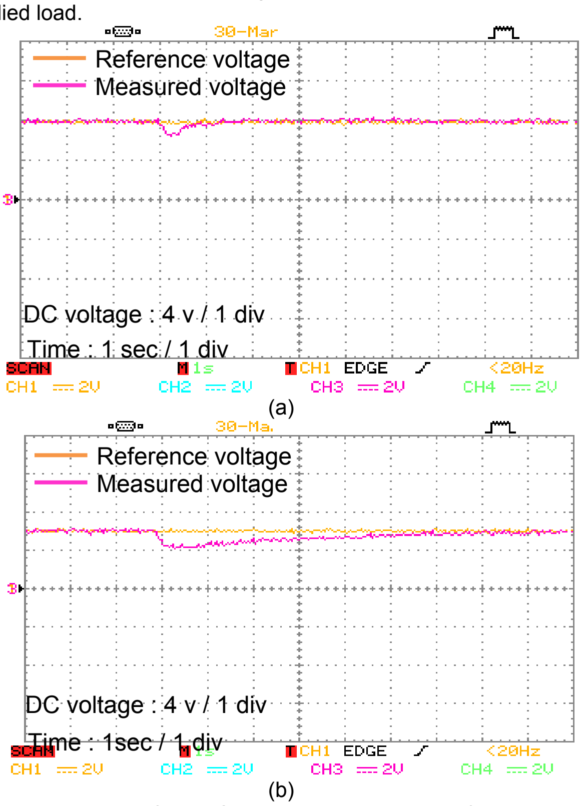

Fig. 12. Response of the DC voltage during a battery fault

Case study 4: Performance with reference in the form of stairs

A reference speed of zero rpm was initially applied at t = 0 seconds, increased to 1200 rpm at t=0.25 s, and 3000 rpm, 3600 rpm at respectively at t = 0.45 seconds, t=0.7 (different level of speed including zero speed regions). It is seen that the speed responses were smooth in different speed zones. We can see that the speed follow perfectly the speed reference.

We note that the performance degrades as approaching the low speed region and fails to provide small oscillations. Figure 13 (b) shows that DC voltage adjustment is assured with slight disturbance. As it is seen from the experimental results, the proposed speed control and power management of electric vehicle motor drives has good performances.

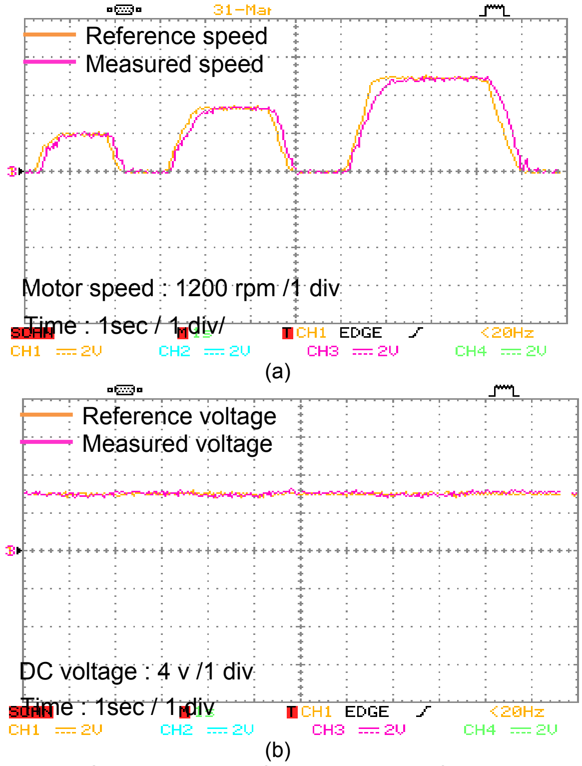

Fig. 13. (a) Speed response for Benchmark reference, (b) DC voltage control.

Conclusion

In this work, the configuration of two DC-DC converters for electric vehicle application to improve energy management has been presented.

A process for the design and development of a unidirectional dc/dc boost buck converters as a module for an electric vehicle. An experimental model was developed using speed control. The control by Lyapunov has a high robustness with very satisfactory regulation performance.

The effects of DC voltage control and the stability of the system were also evaluated and several design decisions were made based on this information. The acceptable operation of the system was verified in buck mode in order to allow for starting the motor. The proposed scheme based boost buck converter fed a Permanent Magnet DC motor for electric vehicle application shows better speed control performance at different operating modes and it keeps the voltage constant for a long time in case of degradation of the performance of the battery. The studied system can be adapted to medium and high power.

APPENDIX

Table 1. Permanent Magnet DC Motor parameters

Components	Rated values and reference
Rated power	60 W
Voltage	6 V, 12V, 24 V
Motor Speed	1733, 6000, 14800 rpm,
Current	0.6 A

Table 2. DC-DC Converters parameters

Components	Rated values and reference
Capacitor	3300μF
Inductance	L=60 mH, r=1.2 Ω
Resistance	1 kΩ
Potentiometer	10 kΩ
MOSFET	IRF530N
Diode	UF 5408
Optocoupler	2N27

Table 3. Battery parameters

Components	Rated values and reference
Voltage	12 V
Capacity	6 Ah

Authors *Rabah Araria, Laboratory of Energy and Computer Engineering L2GEGI, Department of Electrical Engineering, Faculty of Applied Sciences, University of Tiaret, BP 78 Size Zarroura, Tiaret 14000, Algeria, rabah.araria@univ-tiaret.dz.*
Karim Negadi, Laboratory of Energy and Computer Engineering L2GEGI, Department of Electrical Engineering, Faculty of Applied Sciences, University of Tiaret, BP 78 Size Zarroura, Tiaret 14000, Algeria, karim.negadi@univ-tiaret.dz.
Mohamed Boudiaf, Department of Electrical Engineering, University Ziane Achour of Djelfa, Algeria, boudhiaf_mohamed@yahoo.fr.
Fabrizio Marignetti, Dipartimento di Automazione Università degli Studi di Cassino, Italy, marignetti@unicas.it.

REFERENCES

[1] M. Ehsani, Y. Gao, S. Longo, and K. Ebrahimi, Modern electric, hybrid electric, and fuel cell vehicles. *CRC press*, 2018 .
[2] B. Arun, D. Pai, K. N. Chethan, and. al, Review on alternative propulsion in automotives-hybrid vehicles, *International Journal of Engineering and Technology (UAE)*, 7(2018), no. 3, pp. 1311-1319.
[3] Araria R., Negadi K., Marignetti F. Design and analysis of the speed and torque control of IM with DTC based ANN strategy for electric vehicle application, *Tecnica Italiana-Italian Journal of Engineering Science*, 63(2019), No. 2-4, pp.181-188.
[4] Z. Adel, A. A. Hamou, and S. Abdellatif, Design of Real-time PID tracking controller using Arduino Mega 2560for a permanent magnet DC motor under real disturbances, *International Conference on Electrical Sciences and Technologies in Maghreb (CISTEM)*, 2018, pp. 1-5: IEEE.
[5] B. Johansson, DC-DC converters-dynamic model design and experimental verification, 2005
[6] M. Garbarino et al., PID Control Strategies Comparison with Gain Schedule and States Feedback in a Buck-Boost Converter, *IEEE International Conference on Automation/XXIII Congress of the Chilean Association of Automatic Control (ICA-ACCA)*, 2018, pp. 1-6.
[7] H. El Fadil, F. Giri, J. M. Guerrero and A. Tahri, Modeling and Nonlinear Control of a Fuel Cell/Supercapacitor Hybrid Energy Storage System for Electric Vehicles, *IEEE Transactions on Vehicular Technology*, 63(2014), No. 7, pp. 3011-3018,.
[8] E. Hernández-Márquez, and A. C. Avila-Rea, Robust Tracking Controller for a DC/DC Buck-Boost Converter–Inverter–DC Motor System, Energies, 11(2018), No. 10.
[9] A. A. Mahfouz, M. Mohammed, and F. A. Salem, "Modeling, simulation and dynamics analysis issues of electric motor, for mechatronics applications, using different approaches and verification by MATLAB/simulink, *International Journal of Intelligent Systems and Applications*, 5(2013), no. 5, pp. 39.
[10] A. T. Hafez, A. A. Sarhan and S. Givigi, Brushless DC Motor Speed Control Based on Advanced Sliding Mode Control (SMC) Techniques, *IEEE International Systems Conference (SysCon), Orlando, FL, USA*, 2019, pp. 1-6.
[11] Ghosh D, Willich CandKallo J, Development of a novel AC hybrid concept for a fuel cell-battery hybrid electric aircraft with power electronics switches,14th International Conference on Power Electronics (CIEP): IEEE; 2018. p. 105-109.
[12] I. H. Kim and Y. I. Son, Regulation of a DC/DC Boost Converter Under Parametric Uncertainty and Input Voltage Variation Using Nested Reduced-Order PI Observers, *IEEE Transactions on Industrial Electronics*, 64(2017), No. 1, pp. 552-562.
[13] S. Sabzi, M. Asadi and H. Moghbelli, Design and Analysis of Lyapunov Function based Controller for DC-DC Boost Converter, *Indian Journal of Science and Technology*, 9(2016),no 48.
[14] M. Sellali, A. Betka, A. Djerdir,Power management improvement of hybrid energy storage system based on H ∞ control, *Mathematics and Computers in Simulation*, 167(2019), pp. 478-494,